Impact of Hepatic Iron Overload in the Evaluation of Steatosis and Fibrosis in Patients with Nonalcoholic Fatty Liver Disease Using Vibration-Controlled Transient Elastography (VCTE) and MR Imaging Techniques: a Clinical Study

Philippe Pouletaut, Salem Boussida, Redouane Ternifi, Véronique Miette, Stéphane Audière, Céline Fournier, Laurent Sandrin, Fabrice Charleux, Sabine Bensamoun

Impact of Hepatic Iron Overload in the Evaluation of Steatosis and Fibrosis in Patients with Nonalcoholic Fatty Liver Disease Using Vibration-Controlled Transient Elastography (VCTE) and MR Imaging Techniques: a Clinical Study

Philippe Pouletaut[1], Salem Boussida[1], Redouane Ternifi[1], Véronique Miette[2], Stéphane Audière[2], Céline Fournier[2], Laurent Sandrin[2], Fabrice Charleux[3], Sabine F. Bensamoun[1,*]

[1]Sorbonne University, Université de Technologie de Compiègne, UMR CNRS 7338 Biomechanics and Bioengineering, Compiègne, France

[2]Echosens, Département R&D, Paris, France

[3]ACRIM-Polyclinique Saint Côme, Radiologie Médicale, Compiègne, France

[*] Correspondence and requests for materials should be addressed to S.F.B. (Email:sabine.bensamoun@utc.fr)
Université de Technologie de Compiègne (UTC)
Laboratoire Biomécanique et Bioingénierie - UMR CNRS 7338
Rue Roger Couttolenc
CS 60319
60203 Compiègne cedex
France
Tel: (33) 03 44 23 43 90

Highlights

- Complementary imaging modalities are key to evaluate liver fibrosis and steatosis
- Hepatic iron overload is a limitation for US and MR elastographies measurements
- Adaptation of liver MRI protocol to provide quantitative cartography of iron
- Radiologist's awareness on the effect of iron level on the diagnostic result

Graphical Abstract

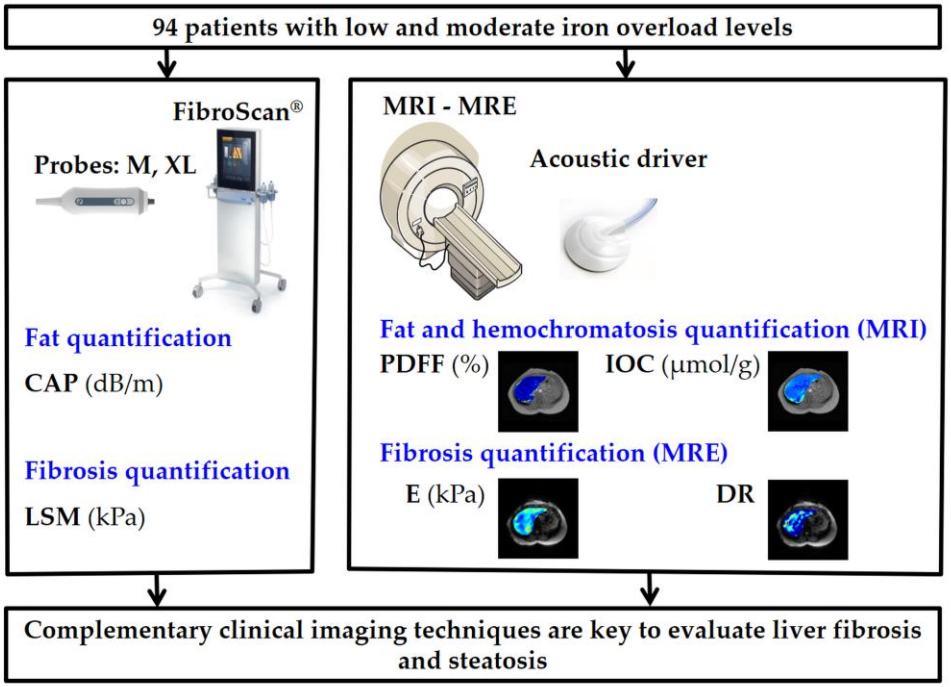

Abstract

Purpose: Three main non-invasive imaging methods are routinely used for the assessment of liver fibrosis and steatosis in patients with nonalcoholic fatty liver disease (NAFLD): the vibration-controlled transient elastography (VCTE) using the FibroScan device, the magnetic resonance imaging (MRI) based on proton density fat fraction (PDFF), and the magnetic resonance elastography (MRE). The purpose of our study is to evaluate the efficiency of the VCTE findings compared to the two others methods, and to analyze the impact of hepatic iron overload on these comparisons.

Methods: A clinical study was performed on 94 patients with NAFLD in the radiology department of ACRIM-Polyclinic Saint-Côme (France). The study also included 17 patients with hemochromatosis, measured from T2* MRI. The liver tissues of all the patients were evaluated with 1) VCTE (including the controlled attenuation (CAP) and stiffness parameters), 2) MRI (fat fraction parameter), and 3) MRE (stiffness parameter) techniques. The performance of VCTE was assessed by estimating the area under the ROC curve (AUC) for patients without or with hemochromatosis. Spearman's correlation was used for the comparison of VCTE measurements to MRI and MRE.

Results: VCTE-based stiffness and CAP were significantly correlated with PDFF and MRE measurements ($P<0.01$) for the subgroup without hemochromatosis. The correlations failed for the subgroup with hemochromatosis.

Conclusion: VCTE and CAP measurements were not correlated with those from MR PDFF and MRE for patients with hemochromatosis. VCTE, PDFF and MRE modalities don't give concordant results for patients with hemochromatosis.

Keywords: attenuation; fat; imaging techniques (elastography, US, MRI); iron; liver; stiffness

1. Introduction

Hepatic fibrosis is routinely controlled in patients with chronic liver disease. The hepatic fibrogenesis can result from several causes, such as high alcohol consumption, chronic viral hepatitis or metabolic dysfunction [1-2]. Steatosis (intracellular fat accumulation) and iron overload are commonly regarded as two important cofactors in liver disease that can lead to fibrosis and cirrhosis [2]. Non-targeted percutaneous liver biopsy with direct histological visualization is the current gold standard to assess liver disease [3], but this technique is invasive and involve potential sampling errors [4].

Thus, three main techniques were emerged for non-invasive detection and quantification of liver fat and iron content. First, a clinically used technique is to measure the stiffness of liver by the vibration-controlled transient elastography (VCTE) using FibroScan® (FS) device [5-6] (Echosens, Paris, France). Ultrasound (US) attenuation measurement using controlled attenuation parameter (CAP) [7] is an additional parameter introduced in 2010 to non-invasively assess liver steatosis [8] and recently improved [9]. CAP measures the attenuation of the ultrasound beam at 3.5 MHz that travels through the liver tissue.

Secondly, magnetic resonance elastography (MRE) was correlated with liver biopsy to validate the imaging method and are now used in clinical routines to evaluate the different stages of stiffness [10].

Third, for iron overload and steatosis quantification, a specific MR sequence called IDEAL-IQ® (Iterative Decomposition of water and fat with Echo Asymmetry and Least squares estimation) demonstrated its clinical relevance [11-12].

The objective of the present work is twice: (i) to compare VCTE (stiffness & CAP) measurements to MRI (PDFF) and MRE (stiffness) values within a NAFLD clinical study and (ii) to evaluate the impact of hepatic iron levels on the measurements of these three non-invasive techniques.

2. Materials and methods

2.1 Study population

Ninety four patients referred for a liver MRI examination were recruited at the radiology department located at the ACRIM-Polyclinique Saint-Côme (Compiègne, France). Each subject underwent 1) FibroScan® examination, 2) MR imaging tests for fat quantification and iron overload, and 3) MR elastography test for viscoelastic characterization with no delay between all the tests (Fig. 1). Total elapsed time for all tests was 10 minutes. Exclusion criteria were claustrophobia, mental instability, or acute reversible liver problems. This study was approved by the Institutional Review Board of Amiens Hospital. All subjects had the experimental protocol explained and gave their informed written consent prior to admission into the study.

Among the study population, 4 were excluded because the CAP files were corrupted. Three patients were also excluded because MRI-PDFF and MRE were not performed. Finally, the study included a total of 87 patients.

2.2 Protocols for fat quantification

(CAP) is measured with the FibroScan® (FS) device using a probe triggered manually by the operator through a standard method [7].

FS is used with two different probes (M and XL) used in function of the thickness of the subcutaneous tissue around the ribcages. The measurement depths and center frequency with M and XL probes are 25-65 mm / 3.5 MHz, and 35-75 mm / 2.5 MHz, respectively.

During the MRI acquisitions the subjects lay supine in a 1.5T Signa HDx MRI machine (GE, Milwaukee, WI) with an abdominal coil. Fat quantification is clinically obtained by applying the standard

IDEAL-IQ® sequence, implemented by General Electric. IDEAL-IQ® is a gradient-echo sequence (TR = 11.5 ms, FA = 7°) applying 6 TEs from 2.4 ms to 9.6 ms. The following parameters were applied: receiver bandwidth = 166.7 kHz, FOV = 26-33 cm, matrix = 160 × 160, slice thickness = 10 mm, 24 slices covering 24 cm in the superior inferior direction. The scan time was approximately 21 s with a single breath-hold. For this study, 32 proton density fat fraction (PDFF) maps were reconstructed from the calculated water-only and fat-only maps (PDFF = fat / (water + fat) × 100). MRI-PDFF region of interest (ROI) was placed in the superior area of liver, at the nearly same location than the ROI of the FibroScan® examination [12], [13], [14].

2.3 Protocols for fibrosis quantification

FS device was used to obtain liver stiffness measurement (LSM), and considered as a reference of stiffness [15]. This imaging technique was preferred to magnetic resonance elastography (MRE) due to the susceptibility artifact in presence of iron. MRE experiments were performed with the MR-Touch® device composed of a clinical acoustic driver for wave generation at 60 Hz, placed at the same level as the diaphragm and set in contact with the ribcage. The applied frequency was chosen according to the analysis by Leclerc et al. [16] who have characterized the material properties of the acoustic driver. Phase images were recorded in one slice with four temporal offsets, a motion sensitizing gradient-echo sequence applied in Z direction, a flip angle of 30°, a field of view between 36 and 48 cm, a 256 × 64 acquisition matrix, a TE/TR equal to 21.7/50 ms. The total scan time was 16 s, corresponding to one breath-holding period.

Viscoelastic maps were generated using multi-model direct inversion (MMDI) [17]. For each dataset, phase images were unwrapped using a minimum discontinuity algorithm and filtered with a Butterworth bandpass (from 2 to 128 waves per FOV) to remove longitudinal waves and noise. Assuming the liver is homogeneous, isotropic, and incompressible, the complex shear modulus $G^* = G' + iG''$ (G': storage modulus, G'': loss modulus) was calculated with a liver density of 1000 kg/m^3. The mean and the standard deviation of Young's modulus $E = 3\,|G^*|$ and damping ratio (DR) = $G'' / (2G')$ were estimated in each ROI. The damping ratio is a relative parameter (viscous to elastic behavior) that was demonstrated to be associated with inflammation [9, 18]. For the DR and E maps, confidence threshold masks were used to evaluate the validity of the pixel values in the ROI [17]: the criterion of ROI placement (circular region of 316 pixels) was such that all pixels in the ROI have a confidence value higher than 80 %.

2.4 MRI protocol for iron overload quantification

The originality of the present study has been to use the IDEAL-IQ® fat sequence to quantify iron volumetrically through the 32 R2* liver slices which are not used in clinical practice. The advanced IDEAL-IQ® protocol used the 32 R2* (1/T2*) liver slices, recorded with a scale unit in Hz, and transformed in iron overload concentration (IOC) in µmol/g with the Wood equation applied to each pixel (IOC = 0.4535/T2* + 3.607 with T2* in second [3]. This advanced IDEAL-IQ® protocol thus provides a volume representation of IOC values in µmol/g. A ROI was placed at the nearly same location than the ROI of the FibroScan®.

2.5 Statistical analysis and staging levels

For descriptive statistics, continuous variables were expressed as medians (interquartile range [IQR]) followed by Mann-Whitney test. Categorical data were summarized as counts. In order to estimate the diagnostic accuracy of VCTE measurements, the analysis was focused on fibrosis threshold F ≥ F2 with gradation obtained by VCTE as reference [15], and on steatosis S ≥ S1 with gradation obtained with MRI-PDFF as reference. The F2 threshold is set to 8.2 kPa for the Young's modulus (E) according to the stiffness thresholds used in VCTE [15]. The S1 threshold is set to 5 % as specified by Tang et al. 2015

[19]. Moreover, the patients were classified in two groups according to the IOC level [4]: hemochromatosis stage H0 for IOC < 36 µmol/g and stage H1 for 36 µmol/g ≤ IOC < 80 µmol/g. An area under the receiver operating characteristic curve (AUROC) is calculated to evaluate the diagnostic performance. The correlation between the different variables (LSM, E, DR, CAP, PDFF) was analyzed using the Spearman's correlation. The conventional level of statistical significance of 0.05 was used for all the analyses.

All statistical computations were performed using the R software version 4.0.3 (The R Foundation for Statistical Computing, Vienna, Austria) and the graphics, stats, pROC, ggplot2 packages.

3. Results

3.1 Patients characteristics and relationships between VCTE and MRI/MRE measurements

The characteristics of the study cohort are provided in Table I. Seventy patients have no hemochromatosis. The IOC value is significantly different between H0 group and H1 group. The Young's modulus (E) value estimated from MRE is also different between these two groups.

The correlation between VCTE and MRI/MRE measurements are summarized in table 2 for the two groups H0 and H1. Of note, for H0 group, there is a significant correlation between LSM and E or DR, whereas there is no corresponding correlation for H1 group. For H0 group, CAP value is correlated to PDFF whereas it is not correlated for H1 group. CAP value is correlated to DR for H1 group.

3.2 Analysis of VCTE measurements of patients without hemochromatosis

The subgroup H0 of patients without hemochromatosis (n=70) include patients with different levels of fibrosis classified as followed: F0-F1 (n = 56), F2 (n = 4), F3 (n = 4) and F4 (n = 6). Among the cohort, there are 29 patients with S0 steatosis stage and 41 patients with S1 steatosis stage.

The results of VCTE measurements are presented in Fig. 2. No significant difference in LSM measurements was found between the two types of probes (Fig. 2A), and the LSM values increase in function of the level of fibrosis stage. CAP measurements with the probe XL are significantly higher for patients with steatosis grade S ≥ S1 (Fig. 2B). This finding results from the specific design of this probe for obese patients. The CAP values increase with the level of steatosis.

Fig. 3 shows ROC curves for the MRE-E and CAP measurements. Young's modulus E identified patients with fibrosis with an AUROC of 0.78 (95% confidence interval [CI] 0.63-0.93) for F ≥ F2 with VCTE as reference. CAP identified patients with steatosis with an AUROC of 0.80 (95% [CI] 0.70-0.91) for S ≥ S1 with PDFF as reference. These findings as well as the significant correlations for LSM vs E and CAP vs PDFF (Table 2), demonstrate the good performance of VCTE measurements for patients without hemochromatosis.

Fig. 4 shows the cartographies of IOC, E, DR and PDFF for the H0 group with different stages of fibrosis and steatosis. It can be observed that the PDFF cartographies show a sparse diffusion of the steatosis for the stage S1 compared to the stage S0.

3.3 Analysis of VCTE measurements of patients with hemochromatosis

The subgroup H1 of patients with hemochromatosis (n = 17) include patients with F0-F1 (n = 14), F2 (n = 1) and F4 (n = 2) fibrosis stage. Among the 17 patients, there are 4 patients with a S0 steatosis stage and 13 patients with a S1 steatosis stage.

Fig. 5 shows the distribution of LSM and CAP measurements. Due to the lack of hemochromatosis patients with a severe fibrosis, the effect of the probe has not been tested on the VCTE parameters.

Table II has revealed no significant correlation for LSM vs E and low correlation for CAP vs PDFF (p = 0.07) for H1 subgroup. Thus, no ROC analysis was performed for fibrosis evaluation. CAP identified

patients with steatosis with an AUROC of 0.71 (95% [CI] 0.45-0.98) for S ≥ S1 with PDFF as reference.

Fig. 6 shows the cartographies of IOC, E, DR and PDFF for patients with different stages of fibrosis and steatosis. The IOC cartographies well represent the heterogeneous distribution of iron compared to the IOC cartographies for the H0 group (Fig. 4). Moreover, the PDFF cartographies illustrate the spatial localization of the steatosis even though for high IOC level.

4. Discussion

The originality of this study was to show the impact of iron on the *in vivo* liver measurements to monitor the fibrosis and / or the steatosis. While it is difficult to recruit hemochromatosis patients, these results will increase radiologist's awareness on the effect of IOC level on the diagnostic result.

The present findings indicate that MRE does not significantly correlate with LSM measurements for patient with hemochromatosis H1 stage. This may be due to the fact that MRE technique is less precise when iron level is too high. Indeed, studies have demonstrated that the gradient-echo sequence used in MRE technique is inaccurate for T2* < 10 ms [20]. In this study, H1 patients have an IOC level superior to 36 µmol/g, corresponding to a T2* value less than 14 ms. As a consequence, from our measurements, we cannot evaluate the effectiveness of MRE for patients with hemochromatosis. A solution would be to use a spin-echo or spin-echo echo-planar imaging MRE sequences [21-22] to give more reliable measurements of stiffness. But this sequence is less widespread in clinical routine due to the high time of acquisition. Otherwise, it may therefore be necessary to resort back to liver biopsy to assess fibrosis in such patients.

In this study, biopsy, considered as the clinical gold standard, was impractical to obtain and VCTE-assessed LSM was chosen as the reference of fibrosis. This imaging biomarker may be controversial as many studies tend to outline a better performance of the MRE technique compared to ultrasound based elastography, including transient elastography [23-24]. Thus, another ROC analysis has been undertaken with MRE as the reference of fibrosis: the F2 threshold is set to 9.9 kPa for the Young's modulus (E) according to the stiffness thresholds used in MRE [17]. The results were similar with an AUROC value of 0.77 (95% confidence interval [CI] 0.62-0.92) compared to 0.78 (95% confidence interval [CI] 0.63-0.93) obtained with VCTE technique as the reference. For the present cohort, the results of the ROC analysis of fibrosis are equivalent.

Concerning the steatosis results, the CAP has low performances in differentiating the steatosis stages for H1 hemochromatosis patients. This observation may be biased by the low number of patients in each group (S0: n = 4; S1: n = 13) and highlight a limitation of the study. It would be of interest to test the new CAP measurements and see whether the findings are the same [8].

The perspectives will be 1) to increase the number of patients with hemochromatosis to confirm the steatosis and fibrosis analysis and 2) to improve the CAP and MRE methods of measurement.

5. Conclusions

The study demonstrates relative good correlations between VCTE and MRI-MRE measurements for patients without hemochromatosis. However, the correlations are degraded for H1 patients with hemochromatosis. This information is of importance for the radiologist and it can be concluded that these non-invasive techniques are well validated for patients with a low level of iron (e.g. IOC < 36 µmol/g).

Conflict of interest statement

All authors have no conflict of interest to disclose.

Financial support

This study was funded by Echosens company (Paris, France).

References

[1] Friedman SL. Mechanisms of Hepatic Fibrogenesis. *Gastroenterology*. 2008;134(6):1655-1669. doi:10.1053/j.gastro.2008.03.003

[2] Reeder SB, Sirlin CB. Quantification of Liver Fat with Magnetic Resonance Imaging. *Magnetic Resonance Imaging Clinics of North America*. 2010;18(3):337-357. doi:10.1016/j.mric.2010.08.013

[3] Gandon Y, Olivié D, Guyader D, et al. Non-invasive assessment of hepatic iron stores by MRI. *The Lancet*. 2004;363(9406):357-362. doi:10.1016/S0140-6736(04)15436-6

[4] Merat S, Sotoudehmanesh R, Nouraie M, et al. Sampling Error in Histopathology Findings of Nonalcoholic Fatty Liver Disease: A Post Mortem Liver Histology Study. *Arch Iran Med*. 2012;15(7):0-0.

[5] Sandrin L, Fourquet B, Hasquenoph JM, et al. Transient elastography: a new noninvasive method for assessment of hepatic fibrosis. *Ultrasound in Medicine & Biology*. 2003;29(12):1705-1713. doi:10.1016/j.ultrasmedbio.2003.07.001

[6] Tapper EB, Castera L, Afdhal NH. FibroScan (Vibration-Controlled Transient Elastography): Where Does It Stand in the United States Practice. *Clinical Gastroenterology and Hepatology*. 2015;13(1):27-36. doi:10.1016/j.cgh.2014.04.039

[7] Sasso M, Beaugrand M, de Ledinghen V, et al. Controlled Attenuation Parameter (CAP): A Novel VCTE™ Guided Ultrasonic Attenuation Measurement for the Evaluation of Hepatic Steatosis: Preliminary Study and Validation in a Cohort of Patients with Chronic Liver Disease from Various Causes. *Ultrasound in Medicine & Biology*. 2010;36(11):1825-1835. doi:10.1016/j.ultrasmedbio.2010.07.005

[8] Audière S, Labourdette A, Miette V, et al. Improved Ultrasound Attenuation Measurement Method for the Non-invasive Evaluation of Hepatic Steatosis Using FibroScan. *Ultrasound in Medicine & Biology*. 2021;47(11):3181-3195. doi:10.1016/j.ultrasmedbio.2021.07.007

[9] Yin Z, Murphy MC, Li J, et al. Prediction of nonalcoholic fatty liver disease (NAFLD) activity score (NAS) with multiparametric hepatic magnetic resonance imaging and elastography. *Eur Radiol*. 2019;29(11):5823-5831. doi:10.1007/s00330-019-06076-0

[10] Bensamoun SF, Leclerc GE, Debernard L, et al. Cutoff Values for Alcoholic Liver Fibrosis Using Magnetic Resonance Elastography Technique. *Alcoholism: Clinical and Experimental Research*. 2013;37(5):811-817. doi:10.1111/acer.12025

[11] Reeder SB, Robson PM, Yu H, et al. Quantification of hepatic steatosis with MRI: The effects of accurate fat spectral modeling. *Journal of Magnetic Resonance Imaging*. 2009;29(6):1332-1339. doi:10.1002/jmri.21751

[12] Kühn JP, Hernando D, Muñoz del Rio A, et al. Effect of Multipeak Spectral Modeling of Fat for Liver Iron and Fat Quantification: Correlation of Biopsy with MR Imaging Results. *Radiology*. 2012;265(1):133-142. doi:10.1148/radiol.12112520

[13] Bensamoun SF, Wang L, Robert L, Charleux F, Latrive JP, Ho Ba Tho MC. Measurement of liver stiffness with two imaging techniques: Magnetic resonance elastography and ultrasound elastometry. *Journal of Magnetic Resonance Imaging*. 2008;28(5):1287-1292. doi:10.1002/jmri.21523

[14] Ternifi R, Pouletaut P, Sasso M, Miette V, Charleux F, Bensamoun SF. Improvements of Liver MR Imaging Clinical Protocols to Simultaneously Quantify Steatosis and Iron Overload. *IRBM*. 2018;39(3):219-225. doi:10.1016/j.irbm.2018.04.004

[15] Eddowes PJ, Sasso M, Allison M, et al. Accuracy of FibroScan Controlled Attenuation Parameter and Liver Stiffness Measurement in Assessing Steatosis and Fibrosis in Patients With Nonalcoholic Fatty Liver Disease. *Gastroenterology*. 2019;156(6):1717-1730. doi:10.1053/j.gastro.2019.01.042

[16] Leclerc GE, Debernard L, Foucart F, et al. Characterization of a hyper-viscoelastic phantom mimicking biological soft tissue using an abdominal pneumatic driver with magnetic resonance elastography (MRE). *Journal of Biomechanics*. 2012;45(6):952-957. doi:10.1016/j.jbiomech.2012.01.017

[17] Silva AM, Grimm RC, Glaser KJ, et al. Magnetic resonance elastography: evaluation of new inversion algorithm and quantitative analysis method. *Abdom Imaging*. 2015;40(4):810-817. doi:10.1007/s00261-015-0372-5

[18] Yin M, Glaser KJ, Manduca A, et al. Distinguishing between Hepatic Inflammation and Fibrosis with MR Elastography. *Radiology*. 2017;284(3):694-705. doi:10.1148/radiol.2017160622

[19] Tang A, Desai A, Hamilton G, et al. Accuracy of MR Imaging–estimated Proton Density Fat Fraction for Classification of Dichotomized Histologic Steatosis Grades in Nonalcoholic Fatty Liver Disease. *Radiology*. 2015;274(2):416-425. doi:10.1148/radiol.14140754

[20] Ghoz HM, Kröner PT, Stancampiano FF, et al. Hepatic iron overload identified by magnetic resonance imaging-based T2* is a predictor of non-diagnostic elastography. *Quantitative Imaging in Medicine and Surgery*. 2019;9(6):92127-92927.

[21] Mariappan YK, Dzyubak B, Glaser KJ, et al. Application of Modified Spin-Echo–based Sequences for Hepatic MR Elastography: Evaluation, Comparison with the Conventional Gradient-Echo Sequence, and Preliminary Clinical Experience. *Radiology*. 2017;282(2):390-398. doi:10.1148/radiol.2016160153

[22] Wang J, Glaser KJ, Zhang T, et al. Assessment of Advanced Hepatic MR Elastography Methods for Susceptibility Artifact Suppression in Clinical Patients. *J Magn Reson Imaging*. 2018;47(4):976-987. doi:10.1002/jmri.25818

[23] Imajo K, Kessoku T, Honda Y, Tomeno W, Ogawa Y, Mawatari H, Fujita K, Yoneda M, Taguri M, Hyogo H, Sumida Y, Ono M, Eguchi Y, Inoue T, Yamanaka T, Wada K, Saito S, Nakajima A. Magnetic Resonance Imaging More Accurately Classifies Steatosis and Fibrosis in Patients With Nonalcoholic Fatty Liver Disease Than Transient Elastography. *Gastroenterology*. 2016;150(3):626-37 e7. Epub 2015/12/19. doi: 10.1053/j.gastro.2015.11.048. PubMed PMID: 26677985.

[24] Park CC, Nguyen P, Hernandez C, Bettencourt R, Ramirez K, Fortney L, Hooker J, Sy E, Savides MT, Alquiraish MH, Valasek MA, Rizo E, Richards L, Brenner D, Sirlin CB, Loomba R. Magnetic Resonance Elastography vs Transient Elastography in Detection of Fibrosis and Noninvasive Measurement of Steatosis in Patients With Biopsy-Proven Nonalcoholic Fatty Liver Disease. *Gastroenterology*. 2017;152(3):598-607 e2. Epub 2016/12/03. doi: 10.1053/j.gastro.2016.10.026. PubMed PMID: 27911262; PMCID: 5285304.

Tables Captions List

Table 1

Hemochromatosis stage	H0	H1
No. of patients	70	17
No. of men	34	15
Age, mean ± SD (y)	57 ± 15	57 ± 15
BMI, mean ± SD (kg/m²)	27 ± 5	25 ± 5
Normal weight/overweight/obese	23 / 17 / 20	11 / 1 / 5
M probe / XL probe	47 / 23	16 / 1
IOC, median (IQR) (µmol/g)	22.8 (6.6)	48.8 (18.4)***
MRE-E, median (IQR) (kPa)	7.52 (3.70)	5.54 (2.78)**
MRE-DR, median (IQR)	0.17 (0.07)	0.15 (0.05)
LSM, median (IQR) (kPa)	5.30 (3.20)	5.20 (2.30)
MRI-PDFF, median (IQR) (%)	5.7 (9.5)	6.9 (12.0)
CAP, median (IQR) (dB/m)	257 (91)	278 (87)

BMI = body mass index; CAP = controlled attenuation parameter; IOC = iron overload concentration; IQR = interquartile range; MRE-DR = damping ratio from magnetic resonance elastography; MRE-E = Young's modulus from magnetic resonance elastography; MRI-PDFF = proton density fat fraction from magnetic resonance imaging; SD = standard deviation. The significant test of the measurement difference is performed with a Mann-Whitney's t-test (**p <0.01, ***p <0.001).

Table 2

Hemochromatosis stage	H0	H1
No. of patients	70	17
Spearmann correlations		
LSM vs E	r = 0.49 (p < 0.001)	r = 0.13 (p = 0.62)
LSM vs DR	r = 0.28 (p < 0.02)	r = 0.25 (p = 0.35)
CAP vs PDFF	r = 0.64 (p < 0.001)	r = 0.46 (p = 0.07)
CAP vs DR	r = 0.15 (p = 0.21)	r = 0.52 (p < 0.04)

CAP = controlled attenuation parameter; DR = damping ratio; E = Young's modulus from magnetic resonance elastography; LSM = liver stiffness measurement; PDFF = proton density fat fraction from magnetic resonance imaging.

Figures Captions List

Fig. 1. Summary of measurements performed on patient with Fibroscan®, MRI and MRE devices. CAP = controlled attenuation parameter; DR = damping ratio; E = Young's modulus from magnetic resonance elastography; LSM = liver stiffness measurement; MRE = magnetic resonance elastography; MRI = magnetic resonance imaging; PDFF = proton density fat fraction from magnetic resonance imaging.

Fig. 2. Distribution of VCTE measurements obtained with M and XL probes for patients without hemochromatosis with different stages of fibrosis (F) and steatosis (S) classified as followed : F < F2 (n = 56), F ≥ F2 (n = 14), S < S1 (n = 29), S ≥ S1 (n = 41). **A.** Liver stiffness measurement (LSM). **B.** Controlled attenuation parameter (CAP). The significant test of the measurement difference between probes is performed with a Mann-Whitney's t-test (**p <0.01).

Fig. 3. Receiver operating curve (ROC) analysis for the subgroup without hemochromatosis and for fibrosis (F) stage greater than or equal to F2 (8.2 kPa, n = 14) and for steatosis (S) stage greater than or equal to S1 (5%, n = 41). **A.** ROC analysis of Young's modulus (E) obtained with MRE. **B.** ROC analysis of CAP. AUROC (95% confidence interval CI): area under the receiver operating characteristic curve.

Fig. 4. Representation of the different cartographies obtained with the MRI (**A.** IOC, **D.** PDFF) and MRE (**B.** Young's modulus, **C.** Damping Ratio map) acquisitions for the H0 group of patient at different fibrosis (F) stages and steatosis (S) stages. 80% confidence threshold masks are superimposed on Young's modulus and Damping Ratio maps.

Fig. 5. Distribution of VCTE measurements obtained with M and XL probes for patients with hemochromatosis with different fibrosis (F) stages and steatosis (S) stages: F < F2 (n = 14), F ≥ F2 (n = 3), S < S1 (n = 4), S ≥ S1 (n = 13). **A.** Liver stiffness measurement (LSM). **B.** Controlled attenuation parameter (CAP). The significant test of the measurement difference between probes is performed with a Mann-Whitney's t-test (**p < 0.01). In this distribution, only one patient was examined with XL probe for the stages F < F2 and S ≥ S1.

Fig. 6. Representation of the different cartographies obtained with the MRI (A. IOC, D. PDFF) and MRE (B. Young's modulus, C. Damping Ratio map) acquisitions for the H1 group of patients at different fibrosis (F) stages and steatosis (S) stages. 80% confidence threshold masks are superimposed on Young's modulus and Damping Ratio maps.

Fig. 1

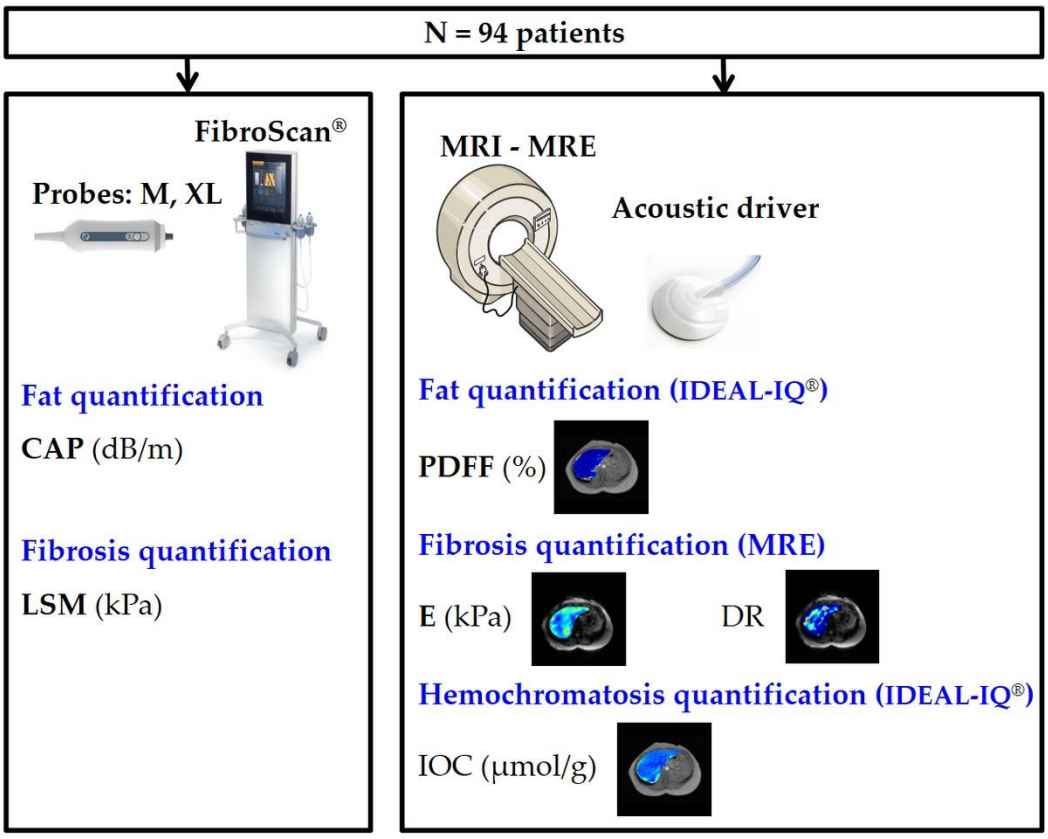
N = 94 patients
FibroScan®
Probes: M, XL
Fat quantification
CAP (dB/m)
Fibrosis quantification
LSM (kPa)
MRI - MRE
Acoustic driver
Fat quantification (IDEAL-IQ®)
PDFF (%)
Fibrosis quantification (MRE)
E (kPa)
DR
Hemochromatosis quantification (IDEAL-IQ®)
IOC (µmol/g)

Fig. 2

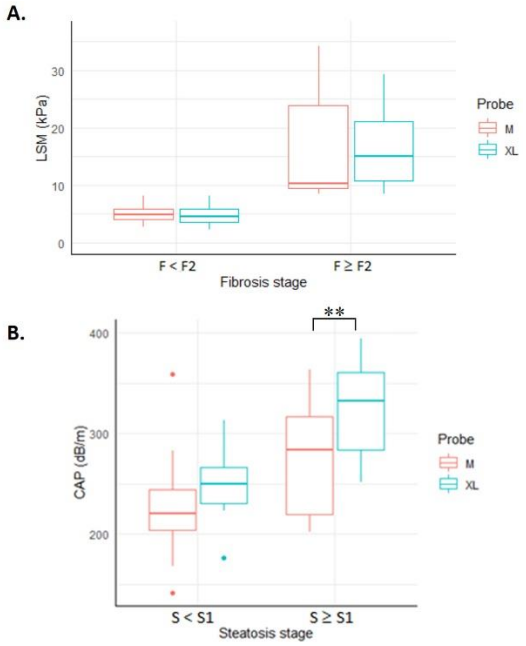
A.
LSM (kPa)
30
20
10
0
F < F2
F ≥ F2
Fibrosis stage
Probe
M
XL
B.
**
CAP (dB/m)
400
300
200
S < S1
S ≥ S1
Steatosis stage
Probe
M
XL

Fig. 3

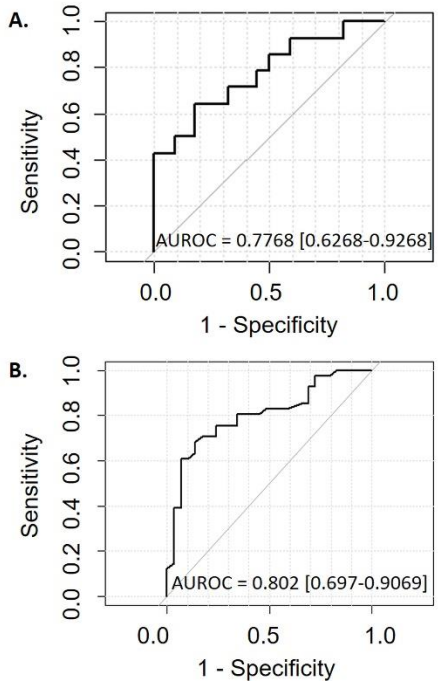
A.
Sensitivity
0.0
0.2
0.4
0.6
0.8
1.0
AUROC = 0.7768 [0.6268-0.9268]
0.0
0.5
1.0
1 - Specificity
B.
Sensitivity
0.0
0.2
0.4
0.6
0.8
1.0
AUROC = 0.802 [0.697-0.9069]
0.0
0.5
1.0
1 - Specificity

Fig. 4

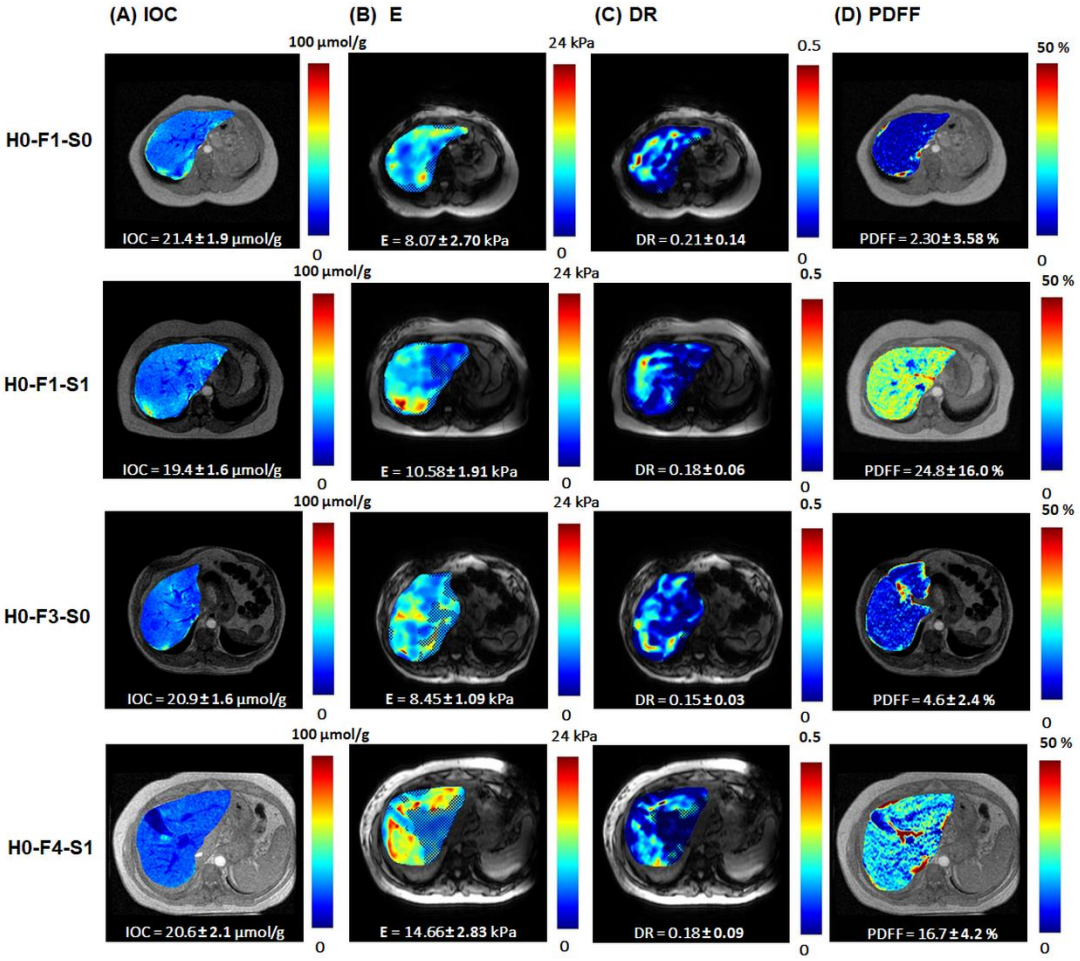
(A) IOC
(B) E
(C) DR
(D) PDFF
H0-F1-S0
H0-F1-S1
H0-F3-S0
H0-F4-S1
100 µmol/g
24 kPa
0.5
50 %
0
IOC = 21.4 ± 1.9 µmol/g
E = 8.07 ± 2.70 kPa
DR = 0.21 ± 0.14
PDFF = 2.30 ± 3.58 %
IOC = 19.4 ± 1.6 µmol/g
E = 10.58 ± 1.91 kPa
DR = 0.18 ± 0.06
PDFF = 24.8 ± 16.0 %
IOC = 20.9 ± 1.6 µmol/g
E = 8.45 ± 1.09 kPa
DR = 0.15 ± 0.03
PDFF = 4.6 ± 2.4 %
IOC = 20.6 ± 2.1 µmol/g
E = 14.66 ± 2.83 kPa
DR = 0.18 ± 0.09
PDFF = 16.7 ± 4.2 %

Fig. 5

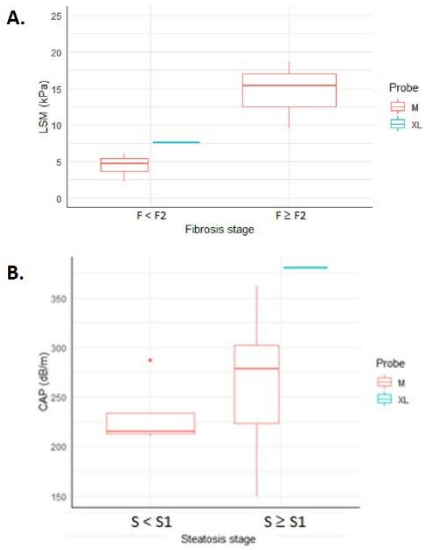
A.
LSM (kPa)
25
20
15
10
5
0
F < F2
F ≥ F2
Fibrosis stage
Probe
M
XL
B.
CAP (dB/m)
350
300
250
200
150
S < S1
S ≥ S1
Steatosis stage
Probe
M
XL

Fig. 6

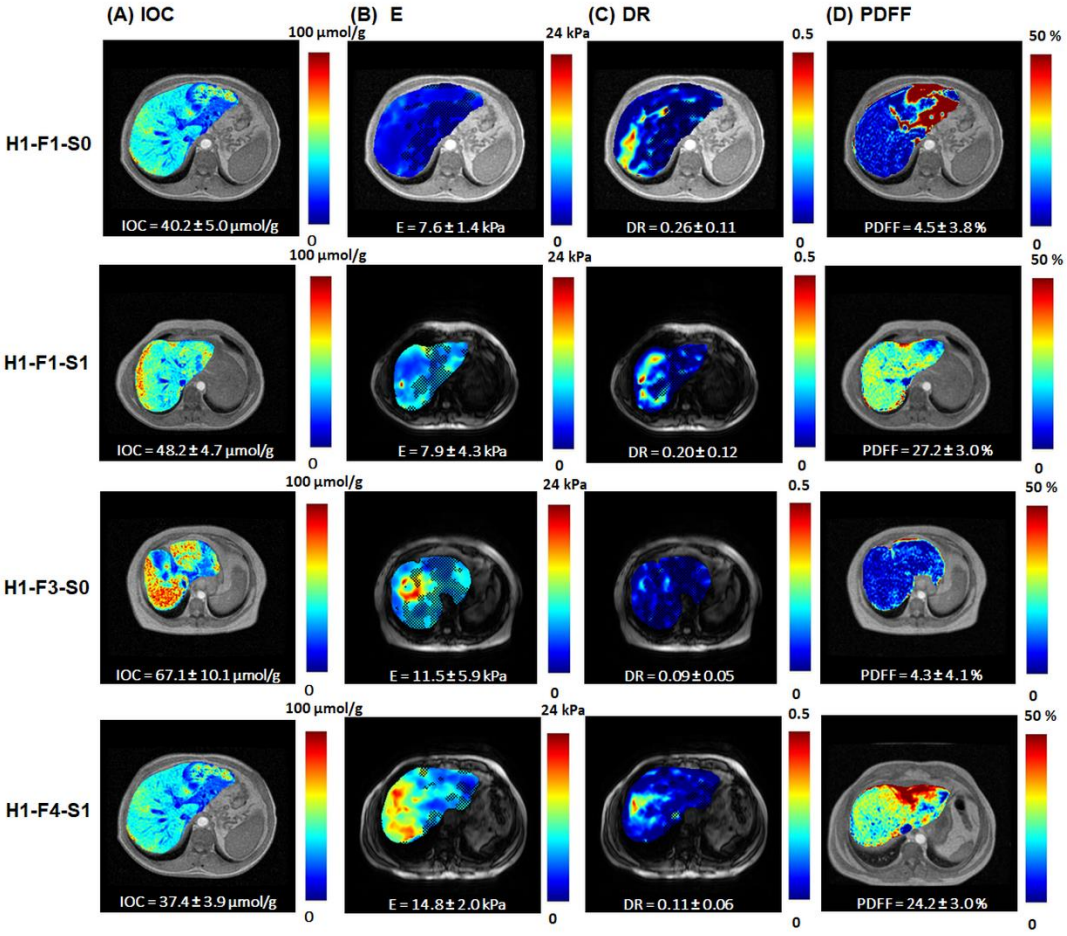
(A) IOC
(B) E
(C) DR
(D) PDFF
H1-F1-S0
H1-F1-S1
H1-F3-S0
H1-F4-S1
100 µmol/g
0
24 kPa
0.5
50 %
IOC = 40.2 ± 5.0 µmol/g
E = 7.6 ± 1.4 kPa
DR = 0.26 ± 0.11
PDFF = 4.5 ± 3.8%
IOC = 48.2 ± 4.7 µmol/g
E = 7.9 ± 4.3 kPa
DR = 0.20 ± 0.12
PDFF = 27.2 ± 3.0%
IOC = 67.1 ± 10.1 µmol/g
E = 11.5 ± 5.9 kPa
DR = 0.09 ± 0.05
PDFF = 4.3 ± 4.1%
IOC = 37.4 ± 3.9 µmol/g
E = 14.8 ± 2.0 kPa
DR = 0.11 ± 0.06
PDFF = 24.2 ± 3.0%